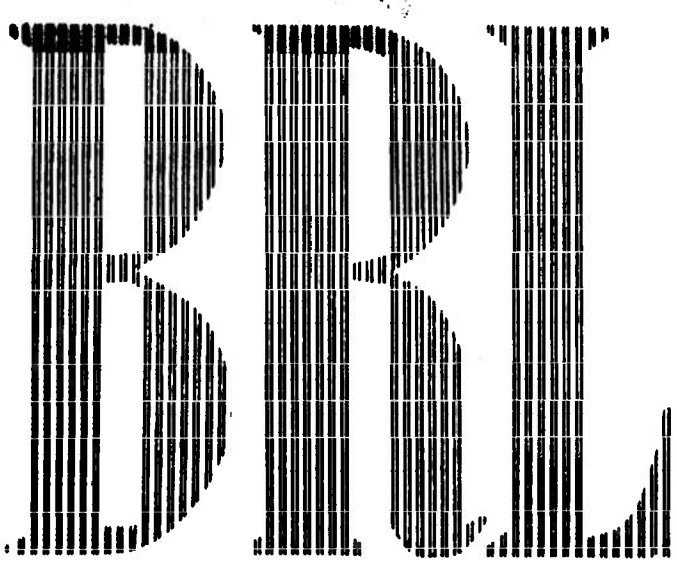

REPORT NO. 1161
FEBRUARY 1962

SHOCK PRODUCING MECHANISMS FOR EXPLODING WIRES

F. D. Bennett

Department of the Army Project No. 503-03-001
Ordnance Management Structure Code No. 5010.11.814

BALLISTIC RESEARCH LABORATORIES

ABERDEEN PROVING GROUND, MARYLAND

B A L L I S T I C R E S E A R C H L A B O R A T O R I E S

REPORT NO. 1161

FEBRUARY 1962

SHOCK PRODUCING MECHANISMS FOR EXPLODING WIRES

F. D. Bennett

Exterior Ballistics Laboratory

Department of the Army Project No. 503-03-001
Ordnance Management Structure Code No. 5010.11.814

A B E R D E E N P R O V I N G G R O U N D, M A R Y L A N D

B A L L I S T I C R E S E A R C H L A B O R A T O R I E S

REPORT NO. 1161

FDBennett/iv
Aberdeen Proving Ground, Md.
February 1962

SHOCK PRODUCING MECHANISMS FOR EXPLODING WIRES

ABSTRACT

Single fringe interferograms are presented of 4-mil Cu wires exploded at 20 kv into argon at ambient pressures of 1/8, 1/16 and 1/32 atm. Features discernible include a compressive head shock wave, arc plasma, a weak plasma wave and the expanding metal wire. On the basis of certain plausible assumptions it is seen that the arc plasma has a temperature of about 2.5 ev; but its leading edge, a region not in thermal equilibrium, has electron temperatures $\sim 10^2$ ev and is the boundary of an electron driven shock wave.

Page intentionally blank

INTRODUCTION

In a recent application of interferometric techniques[1*], the formation of shock waves by exploding wires at low ambient densities of argon, c. 1/16 atm, is shown to depend on the formation and expansion of an arc plasma concentric with the wire. The interferograms presented there are all of the multi-fringe type most useful for the existing schemes of quantitative reduction. Certain features of the flow are readily discerned in a multiple fringe picture, but others remain hidden from view because of the discontinuous mapping of the disturbance offered by the light or dark fringes. By a slight modification of technique to employ a single fringe field, a different representation of the flow can be achieved which exhibits certain finer details not easily detectable in the multiple fringe pictures. The present study is concerned with a semi-quantitative analysis of single-fringe interferograms from wire explosions in argon, taken under conditions corresponding to those of the multiple fringe interferograms presented in our previous paper.

* This paper will hereafter be designated by [1].

Page intentionally blank

2. EXPERIMENTAL DATA

2.1 Interferograms.

The general technique is described in [1]. To obtain a single fringe interferogram one need only increase the fringe spacing until a single light or dark fringe, preferably one of the central fringes in the pattern, uniformly covers the entire field of the interferometer. Plate imperfections may prevent perfectly uniform illumination of the field, but are evident mainly at the edges and need not concern us when the disturbance is reasonably well centered. With these conditions of adjustment the interferometer shows directly the contours of constant fringe shift, and represents the boundary of the disturbance in a nearly continuous curve. Single fringe interferograms of 4-mil Cu wires at 20 kv exploded in argon at 1/32, 1/16 and 1/8 atm are shown in Figures 1 - 3.

2.2 General Features.

Inspection of these figures and comparison with the earlier multifringe pictures [1] allows certain major phenomena to be readily identified.

The rounded tip, foremost in the streak interferogram, is clearly the boundary of the peripheral arc within which the negative fringe shift achieves its largest magnitude. The zero fringe contour can be seen entering the pattern just outside the arc boundary. It is continuously connected to the undisturbed fringe ahead of the explosion and separates the major area of negative fringe shift near the axis from the area of positive fringe shift further out and just behind the head shock wave. The head shock is the nearly straight, outer boundary of the disturbance.

Numbering light fringes with half integers and dark with whole, it is clear that the contour $\delta = +0.5$ lies just inside the shock on each side of the central axis. Then comes the $\delta = 0$ contour which

originates in the undisturbed field ahead of the explosion, proceeds back and slightly outward only to loop forward again at smaller radii into the compressed region just outside the expanding wire material. In the 1/32-atm case the returning zeroth fringe occupies a large, wedge shaped area closest to the weakly expanding wire. Inside the zeroth contour lies that for $\delta = -0.5$ which outlines the arc, streams backward in time through a broadening area and then returns very sharply near the expanding wire to connect with itself and form a closed loop at the tip. Within it one finds the $\delta = -1.0$ and $\delta = -1.5$ areas both of which lie close to the axis in the region of most intense luminosity. In the 1/8-atm case, luminosity partly obscures the inner, negative fringe contours.

Near the tip of the disturbance, transverse paths of the interferometer beam are small but negative fringe shifts are large. These facts imply high electron densities. At large radii and later times, the paths are longer and smaller electron densities will achieve the same fringe shift. The contour for $\delta = -0.5$ may fairly be taken as the area depicting the onset and decay of the electron cloud. The zeroth contour represents the area in which refraction effects of electrons versus those of compressed ions and atoms just cancel.

Two compressive shocks can be seen. For orientation refer to Figure 4. The first, which we shall call SI, is the head shock wave already noted. The second, SII, is delineated by the sharp boundary near the expanding wire material where fringe shift is positive in passing from $\delta = 0$ to $\delta = -0.5$ with increasing radius. Inside the shock SII, the wire material is seen to expand, weakly in the 1/32-atm case and more strongly in the 1/16- and 1/8-atm cases. In these latter, fringes of rather definite structure can be seen within the metal boundary itself.

Finally, we note a weak disturbance, denoted by WS, originating at the tip where the $\delta = -0.5$ contour first closely approaches the expanding wire (see Figure 2, the 1/16-atm case particularly).

This weak disturbance appears to reflect from the wire and rise steeply along a straight path, causing an outward flare in the $\delta = -0.5$ contour at about $t = 2$ μsec. A little consideration shows that the fringe shift across this disturbance is negative, indicating a detectable increase in electron density.

2.3 Measured Velocities.

In the particular case of the 1/16-atm interferogram, velocity measurements have been made of each of the visible disturbances just cataloged and are presented in Table I, where P stands for the

TABLE I - 1/16 ATM ARGON

Disturbance	P	SI	SII	WS
Velocity (mm/μsec)	> 20	1.5	1.0	4.2
Mach No. (a_o = .32 mm/μsec)	> 60	4.7		

plasm boundary near the tip. Mach numbers have been calculated relative to room temperature argon for purposes of comparison with shock tube data. The velocity of 20 mm/μsec for the plasma boundary P is measured where the front intersects the expanding wire.

2.4 Estimated Energies.

Although it is shown in our previous study [1] that blast wave theory is not strictly applicable to exploding wire shocks, it nevertheless provides a useful way of classifying such shock waves. Accordingly we give here in Table II a list of apparent energies in joules/cm indicated by the sequence of wire explosions into argon, realizing that the values given do not accurately represent the energy in the flow field behind the shock. They do have the heuristic merit of ordering the shocks according to apparent energy. On the basis of our previous study [1] it seems likely that this ordering has validity for $p > 1/4$ atm.

TABLE II

p (atm)	1	1/2	1/4	1/8	1/16
E (joules/cm)	6.2	2.9	1	0.7	0.5

3. ANALYSIS

3.1 Plasma Boundaries.

We have already noticed that the $\delta = -0.5$ fringe gives a crude indication of the extent of the electron cloud in any of the single fringe interferograms. This notion may be made somewhat more precise by observing that the zeroth fringe contour is the locus for which the total path difference, including negative contributions by electrons and positive by compressed ions and atoms, is zero. Near the tip of the disturbance where the zeroth fringe is first seen, the entire light path in the disturbance cannot be distinguished from a path of equal length in the undisturbed beam. Therefore, for this gap in the contour caused by the zeroth fringe, the effects of electrons just cancel those of ions and atoms. A calculation may be made, based on certain reasonable assumptions, which will set an upper bound on the electron concentration at this point. We consider only the 1/16-atm case.

Combining the results for refractivities of argon and of free electrons given by Alpher and White[2], and assuming that ions and atoms have equal refractivities, we can write

$$\mu(\rho) - \mu(\rho_o) = -1.33 \times (10)^{-22} N_e + 2.84 \times 10^{-4} (\rho - \rho_o)/\rho_{STP} \qquad (1)$$

where μ represents refractive index, N_e is electron concentration, ρ and ρ_o are densities in the disturbed and undisturbed beams respectively, ρ_{STP} is the density of argon at standard temperature and pressure, and wavelength $\lambda = 5.46 \times 10^{-5}$ cm has been used in evaluation of the constants.

For an axisymmetric shock it is well known that fringe shift is zero at the shock but rises abruptly, with a vertical tangent just inside, because the path in the disturbance increases rapidly while index jump remains nearly constant. A zero shift through the shock can only be achieved if the difference in in indices vanishes; thus, the left side of Equation (1) is zero at the point in question.

The head shock, SI, is seen from Table I to have $M \approx 5$ and therefore may be considered a strong shock wave. The density jump across such a shock is given by $\rho_2/\rho_1 = (\gamma + 1)/(\gamma - 1)$. With $\gamma = 5/3$ for argon and with $\rho_1 = \rho_o = \rho_{STP}/16$ we can immediately find $N_e = 4 \times 10^{17}$ electrons/cc for the 1/16 atm case. This electron concentration is about the same as that of the first contour exhibited in [1]. Further back along the zeroth fringe, it is plausible that the mean electron concentration must increase continuously to counteract the positive shift caused by the positive index integrated along the increasing transverse path within the shock. Thus the $N_e = 4 \times 10^{17}$ contour should be further and further above the zeroth fringe.*

Nearer the axis and just beyond the expanding wire material, the zeroth fringe appears again, this time as a narrow band bordered on the outside by the $\delta = -0.5$ contour. Here the interpretation in terms of electron densities is difficult because the integrated effects of the compressed ions and neutrals behind the shock SI together with electron effects indicated by the various negative fringe contours must be included to yield the zeroth fringe. Lacking a quantitative analysis, one can argue that the abrupt positive jump of 1/2 fringe at the zeroth fringe boundary represents a compressional shock discontinuity. This is corroborated by the sharply hooked fringes of the corresponding multiple fringe interferograms [1]. The appearance of compressional shock SII, argues that negative shifts caused by electrons at this boundary are negligible. This in turn implies electron densities $N_e < 4 \times 10^{17}/cc$.

The conclusion could be false if SII represents a density jump $\rho_2/\rho_1 > 4$, which could only be accounted for by assuming an appreciable concentration of some massive atomic or molecular species behind the shock, e.g. copper atoms or argon molecule ions A_2^+. The density

*This is easily proven if shock, electron cloud boundary and zeroth contour occur in this order and trace similar power-law curves.

jump is probably not much larger than 4 since at late times $t > 8$ μsec, the SII boundary is broadened and nearly erased by what appears to be an increase in electron concentration. This effect may conceivably be ascribed to increased ionization caused by the relatively weak SII shock as it passes over high temperature argon atoms already in excited states produced by the peripheral arc. The multiple fringe interferograms especially well show this broadening of the boundary and the accompanying luminosity.

3.2 Temperature Behind the Head Shock Wave.

At the time that SI first becomes visible it is clearly nonluminous, as may be further corroborated by inspection of the figures in [1]; furthermore, the argument of the previous paragraph implies that SI lies increasingly outside the contour with $N_e = 4 \times 10^{17}$/cc. Since the shock is compressional and strong ($M \sim 5$), the density immediately behind it is almost $4\,\rho_o$. Thus for the 1/16 atm case the argon atom density is approximately 6×10^{18}/cc and ionization remaining behind the shock should be less than 7%. The shock itself is too weak to cause further ionization unless appreciable numbers of excited argon atoms exist in the undisturbed region. We discount this possibility because of the absence of luminosity. We may therefore regard SI as a strong shock wave propagating into a perfect gas of $\gamma = 5/3$ at room temperature.

With these assumptions, the temperature ratio across a strong shock wave traveling at Mach M_1 is given by $T_2/T_1 = \left[2\gamma(\gamma-1)/(\gamma+1)^2\right] M_1^2$. Substitution shows T_2/T_1 slightly less than 8 and $T_2 \sim 2400\ ^\circ K$.

The shock wave SI is approximately straight in the 1/32 and 1/16 atm cases and therefore proceeds at nearly constant Mach number over most of the field of view. Two inferences may be made: 1) the shock is receiving substantial amounts of energy from the expanding interior regions; otherwise, it would decelerate and show appreciable curvature, and 2) the gas passed over by the shock, roughly bounded inside by the zeroth fringe, is heated at least to the temperature $T_2 \sim 2400^\circ K$.

3.3 Estimate from Blast Wave Theory.

Some doubt may remain whether the head shock wave could conceivably have originated at the expanding wire like a blast wave and remained obscured by the arc plasma until appearing beyond the zeroth fringe contour. The measured properties of the wave are incompatible with such a view as will appear from the following argument.

From the equations of the blast wave theory for cylindrical shocks[3] and the perfect gas law, an expression for temperature ratio across the shock can be found. It is

$$\frac{T_2}{T_1} = \frac{2\gamma(\gamma-1)}{(\gamma+1)^2} \qquad M_1^2 = \frac{2\gamma(\gamma-1)}{(\gamma+1)^2}\left(\frac{E}{4\epsilon\,\rho_o}\right)^{\frac{1}{2}} \frac{1}{a_o^2 t}\,, \tag{2}$$

where the symbols have their usual meaning, t is time and a_o the velocity of sound in the undisturbed medium. The constant $\epsilon = 2.25$ is the result of some improved calculations[4] that furnish values appropriate for argon and correct certain numerical errors in Lin's tabulated functions.

The first equality of (2) occurs because the theory assumes the strong shock conditions at the boundary, and therefore must agree with the result of § 3.2. The second equality expresses the ratio in terms of the time and the constants characterizing the assumed shock wave. Using $E = 0.5 \times 10^7$ ergs/cm from Table II, $\rho_o = .105 \times 10^{-3}$ gms/cc and $a_o = 3.2 \times 10^4$ cm/sec the quantity corresponding to M_1^2 becomes $71/t\,(\mu\text{sec})$. Agreement with the previous value, $M_1^2 \sim 25$, is achieved either by taking $t \sim 3$ μsec or multiplying E by factor 1/9. Either alternative contradicts the observations and must be considered unacceptable as a true description of the shock wave. The first implies an origin in time 2 μsec ahead of that actually observed. The second implies a shock radius R only 1/3 of that observed, through the dependence $R \propto E^{\frac{1}{4}} t^{\frac{1}{2}}$.

This estimate given by blast wave theory indicates convincingly that the head shock SI cannot have originated on the axis at the true, experimental origin in time, a fact we have already appreciated from a different point of view.

3.4 Thermalization Times.

It is of great interest to know whether conditions inside the peripheral arc approach local thermodynamic equilibrium, that is whether electrons, ions and neutrals are closely in local temperature equilibrium or not. For, if so, we may conclude that the head shock wave could be produced by thermal expansion processes of the usual type. If not, we may then consider whether the shock is of the "electron driven" type reported by Fowler et.al[5] where the hot, expanding electron gas draws the cold ions and neutrals with it by means of Coulomb and collisional forces.

In this section we employ known experimental data and theoretical expressions to calculate critical time intervals for approach to thermal equilibrium between electrons, neutrals and ions for various assumed collision processes.

We consider first the conditions which may exist at the edges of the peripheral arc and in the region where the head shock, SI, appears to originate. Our experimental data [1] and previous considerations indicate that the electron density is sufficiently low so that electron-atom collisions may be considered to predominate. Even though electron-electron collisions may occur only once for every 15 electron-atom collisions, because of the great disparity of masses ($2m/M \sim 1/40{,}000$), the electrons lose little energy to the atoms, yet remain in temperature equilibrium themselves.

Making use of the definitions and data presented by Brown[6], we present in Table III the results of calculations for electron-atom collisions in argon. Here V is electron energy in ev, T_e is electron temperature in ^{o}K, v is electron velocity in cm/sec, P_c the average

number of electron-atom collisions per cm of electron travel per mm Hg pressure at $0^{o}C$, $\nu_c = p_o P_c v$ is the electron-atom collision frequency, $p_o = 273\ p/T$ where $p = 47.5$ mm (1/16 atm), $\lambda_e = v/\nu_c$ is the electron mean-free-path and $\tau = 4 \times 10^{4}/\nu_c$ is the average time during which an electron would transfer its energy to atoms i.e. it is assumed to take in the neighborhood of 40,000 electron-atom collisions to bring electrons into thermal equilibrium with atoms.

TABLE III

1/16 ATM ARGON

$V^{\frac{1}{2}}$ ($\sqrt{ev}$)	T_e (^{o}K)	v (cm/sec)	P_c	ν_c coll/sec	λ_e (cm)	τ (μsec)
1	8×10^{3}	0.6×10^{8}	4	0.1×10^{11}	6×10^{-3}	4.0
2	32 " "	1.2 " "	27	1.4 " "	9×10^{-4}	0.3
3	72 " "	1.8 " "	72	5.6 " "	3 " "	0.07
3.5	96 " "	2.1 " "	83	8.0 " "	2.6" "	0.05

Because of the Ramsauer effect in argon, the probability of collision P_c varies by a factor of more than 20 as electron energy goes from 1 to 12. Inspection of the last column indicates a hundred-fold variation in time elapsed to obtain thermal equilibrium between electrons and atoms. One may not conclude that the longer thermalization times prevail, because the axial electric field may be of the order of several kv/cm during the formation of the peripheral arc and for several hundred nanoseconds thereafter[7]. Since it seems unlikely that the average electron energy is less than 2 - 3 ev, we may tentatively conclude that the thermalization time is certainly not longer than the time for appearance of the head shock wave and that the head shock is probably mainly thermal in origin.

As for conditions near the center of the peripheral arc and in regions where the ionization exceeds 10%, we have recourse to theoretical expressions derived for completely ionized plasmas in which collision processes are conditioned on long-range electrical forces.

Making use of Spitzer's Equations (5 - 26) and (5 - 31)[8] we calculate the electron, self-collision time t_c and the equipartition time t_{eq}, between electrons and argon ions. Because of the massiveness of argon ions relative to electrons and less importantly because of the relatively low temperature we assume for the ions initially ($T_1 \sim 300^{\circ}K$), each expression, t_c or t_{eq}, is proportional to $T_e^{3/2}$ and thus increases rapidly with electron temperature. In order to establish what may be an upper bound for these times, we assume the mean electron energy to be about 10 ev ($T_e \sim 10^5\ ^{\circ}K$). Then taking the number density of electrons or ions to be 10^{18}/cc, we obtain $t_c \sim 10^{-12}$ sec and $t_{eq} \sim 5 \times 10^{-8}$ sec. The self-collision time for argon ions at room temperature is larger than that for electrons in the ratio $(40 \times 1823)^{\frac{1}{2}}\ (3 \times 10^{-3})^{3/2}$ and as the temperature of the ions rises toward $10^5\ ^{\circ}K$, the second factor would approach unity. Thus at the outset the self-collision time for argon ions is actually .04 that of electrons but rises to 270 time as much. It never exceeds 10^{-9} sec.

These calculations support the view that initially the electrons and ions are in temperature equilibrium among themselves and come into temperature equilibrium with each other in not longer than 50 nanosec, a time represented by about 1/5 of the first light fringe at the tip of the 1/16-atm interferogram, Figure 2. Thus we should expect conditions within the peripheral arc closely to approximate local thermodynamic equilibrium until the electron density falls to a value, arbitrarily taken here as 10% ionization, below which plasma behaviour can no longer be expected. Even in the outer regions of low ionization, thermalization times for the more energetic electrons are of the order of 50 - 100 nanosec, as may be seen from Table III.

3.5 One-Dimensional Unsteady Flow.

The fact that local thermodynamic equilibrium can be expected from point to point throughout most of the peripheral arc region suggests another approach to estimating the average temperature there.

Let us assume that just prior to the emergence of the shock SI, the annulus of the peripheral arc, which may be considered as nearly a right circular cylinder, contains argon gas at high temperature and pressure but at or near the original undisturbed density. This situation could be realized because of the rapidity of heating and the massiveness of the gas. Then, in the next interval of time, a few tenths μsec, expansion of this heated gas gives rise to the head shock wave. If the outer radius is sufficiently large and the time interval short enough so that the expansion wave propagates only a small distance back into the high temperature reservoir, the results of unsteady flow theory applicable to the one-dimensional shock tube may be used.

Resler et.al.[9] developed an expression for the pressure ratio p_4/p_1 between reservoir pressure p_4 and pressure p_1 in the undisturbed region ahead of the shock. Their Equation (7) is a function of the shock Mach number M_1, the velocities of sound a_1, a_4 and the gas constants γ_1, γ_4. Under the assumption already made that $\rho_1 = \rho_4$, and $\gamma_1 = \gamma_4 = 5/3$ with the perfect gas law and $a = (\gamma \hat{R}T)^{\frac{1}{2}}$, we can obtain an implicit expression for the temperature ratio T_4/T_1 as a function of M_1. A numerical solution of this equation shows that $M_1 \sim 5$ corresponds to $T_4/T_1 \sim 74$. Thus, for our 1/16-atm case the temperature of the heated plasma, before appreciable expansion, is indicated to be about 22,000 $^{\circ}$K. It is interesting to observe that this is the temperature for which Olsen[10] finds a maximum in the conductivity of a thermalized argon plasma at one atmosphere pressure. He observes temperatures of this order near the anode. Increasing total current has the effect of enlarging the arc and the high temperature (20,000 $^{\circ}$K) region near the anode but does not increase the maximum temperature appreciably.

3.6 Sound Speed in the Arc Region.

Close examination of the interferograms for the 1/16- and 1/32-atm cases shows that the weak wave WS originates on the expanding wire surface at the time that the inward expanding arc boundary intersects

the wire. Thence it expands along a nearly straight path which crosses the $\delta = -0.5$ fringe contour and shows a pronounced shift toward larger radii on the downstream, or later time, side. Comparison shows that the fringe shift across WS is negative and suggests that a detectable increase in electron density has occurred. The disturbance is not easily traced into the compressional region behind SI probably because the compressional density change is too weak to detect.

Comparison between the 1/16-atm and higher pressure interferograms shows that the flare in the first negative fringe, with attendant negative fringe shift, can be discerned in several cases. This observation suggests that similar disturbances are present in these also, but cannot be seen at early times because at higher pressures the arc region is much smaller and because luminosity obscures the field of view.

The cause of disturbance WS is not known and not readily inferred. Because it originates from the most rapid arc process and at early enough times so that complete thermalization may not have occurred, the suspicion is aroused that it may be a shock or abrupt disturbance of the "electron driven" category described by Fowler et.al[5].

The facts that the disturbance WS has a moderate velocity, reflects from the dense, metal boundary and causes a slight but detectable increase in electron density suggests that it is hydrodynamical in nature; for a weak shock in a moving, high-temperature gas or plasma could propagate at several times the speed of sound in the ambient cold gas and by compression could slightly increase the temperature and the accompanying ionization in the gas over which it passes.

We shall assume that WS is indeed a weak disturbance and that it propagates in a high temperature plasma which is in local thermodynamic equilibrium. Its velocity relative to the fluid in which it moves is then slightly greater than, or equal to, the wave velocity in the medium.

According to the treatment of positive-ion oscillations which preserve electrical neutrality, given by Spitzer[11], this velocity, for the case of argon plasma is given by $a_p^2 = (2\gamma kT_p)/m_i$ where $m_i = m_A$ is the ionic or atomic mass.

The sound speed in the undisturbed region is just $a_o^2 = (\gamma kT_o)/m_A$; thus we find $2T_p/T_o = (a_p/a_o)^2$. Taking a_p to be the velocity of the weak shock, WS, from Table I and $a_o = 0.32$ mm/μsec, we obtain $T_p/T_o = 86$ or $T_p \sim 26{,}000\ ^oK$. The agreement with our previous estimate, obtained from one-dimensional unsteady flow theory, seems quite satisfactory.

We have not made any allowance for the fact that the fluid supporting WS may be in motion. We may infer that it is in a state or practically uniform motion from the straightness of WS and the absence of other discontinuities.

The inner boundary, SII, is moving at 1 mm/μsec and the outer boundary, SI, at 1.5 mm/usec. If SI had passed over the entire region traversed by WS the velocity of the fluid, given by the strong shock relations would be $2/(\gamma + 1) = 3/4$ times the velocity of the shock.

It seems more likely that only the latter end of WS could be affected by SI and that the fluid traversed by WS is practically at rest. Nevertheless, the above argument makes it appear quite certain that the fluid velocity in the region of WS cannot exceed 1.1 mm/μsec.

If we make this correction to the velocity of WS the temperature estimate becomes $T_p/T_o = 46$ and $T_p \sim 14{,}000\ ^oK$. This value may be regarded as somewhat too low.

The possibility that WS is a magnetohydrodynamic disturbance, dependent on magnetic field, cannot be ruled out but seems unlikely for the following reasons. WS is practically straight throughout a time interval long enough for at least one current (and field) reversal to take place. No corresponding variation in slope of WS can be seen.

Since the current has transferred from the wire to the arc and the current density may be considered reasonably uniform, the magnetic field will rise linearly with radius through much of the region traversed by WS. Strong dependence on magnetic field would argue changing slope of WS which is not observed. We conclude that WS can be at most only weakly dependent on magnetic field and are therefore justified in considering it to be an acoustic wave in the plasma.

3.7 Electron Driven Shock Waves.

According to Fowler et.al.[5] the velocity of the fast luminous front, which they indentify as electron driven, is given by $V^2 \sim k T_e/M$, where T_e is the electron temperature and M is the ion mass. A calculation with $T_e \sim 2.5$ ev, which corresponds to our previous temperature estimates, gives a velocity of 2 mm/μsec. This is comparable with the velocity of WS but considerably smaller than the lower bound on average velocity of P given in Table I. This fact suggests that the effective electron temperature just inside the front surface P may be considerably larger than the value of 2.5 ev which ought to hold in the arc region where ions and electrons are in temperature equilibrium.

We have no independent measure of electron temperature just behind the arc front P, but setting V = 2 cm/μsec as a lower bound yields an electron temperature $T_e \sim 200$ ev in the front. Such a high value forces us to reconsider the estimated collision and equipartition times calculated earlier.

The interferograms and electron contours of [1] show the leading edge of the peripheral arc, in which ionization rises from zero to 10%, to be somewhat less than 1/3 mm in linear dimension and when extrapolated to the tip about 100 nsec in duration. In this narrow border, electron-atom collisions will predominate and calculations like those of Table III may be appropriate.

If we extend the collision cross-section curve for argon[6] with an hyperbolic approximation which fits the high-energy tail quite well, we find that the time τ for electrons and atoms to come to equilibrium

approaches a constant value of about 75 nsec but remains in the range 50 - 80 nsec for electron energies down to 9 ev. These estimates show clearly that as ionization rises through 10% in the arc front, all electrons with energies higher than 9 ev can approach temperature equilibrium with atoms. Those initially at 200 ev will fall rapidly in temperature in the same interval unless energy is continuously added. Because the relative number of electrons is small the resultant mixing temperature will be much lower than the maximum electron temperature. Beyond the 10% ionization contour, plasma conditions will begin to prevail and the estimates of § 3.4 may be used. For $T_e \leq 10$ ev the equipartition time is less than 50 nsec; therefore, in a total time not exceeding 150 nsec we would expect the high-temperature electrons to have cooled and come to thermal equilibrium in the arc plasma. Our previous estimates put the equilibrium temperature at about 2.5 ev.

To summarize, if we regard WS as the reflection of P from the wire boundary, then P is in some ways like a fluid mechanical shock wave. Furthermore, the velocity of P and knowledge of electron densities behind P indicate that in the leading edge of the arc, less than 0.1 μsec wide electron temperatures are of order 200 ev and are far higher than those for the surrounding atoms and ions which were initially at room temperature. We conclude on the basis of the foregoing argument that the assumption that the arc front P is an electron driven shock wave of the type discussed by Fowler and co-authors is compatible with the experimental data and offers a consistent explanation of the leading edge of the arc.

4. SUMMARY

As a sequal to our earlier interferometric study we present single fringe interferograms of exploding copper wires at ambient pressures of 1/8, 1/16, 1/32, atm of argon. Features of the disturbance not easily recognized in multiple fringe pictures stand out clearly. In particular it is possible to distinguish the peripheral arc boundary P, the compressive head shock wave SI, a fast weak disturbance WS and a compressive shock at the expanding boundary of the copper metal SII. Representative velocity values obtained from the 1/16-atm case are used in a semi-quantitative analysis.

The following main points are noted:

a. The fluid disturbance can be divided roughly into three regions; a compression bounded on the outside by the head shock and internally by the zeroth fringe contour; an annular plasma bounded by the zeroth fringe contour and internally by the expanding wire; and the expanding wire vapor, itself the nearest of the regions to the axis.

b. Strong-shock-wave, boundary conditions indicate that temperature behind the head shock is about 2500 ^{o}K. Application of blast wave theory confirms that the flow is still gaining energy during the time of observation and that it originates not at the wire surface but on an annulus about 1 cm in diameter formed by the expanding peripheral arc. Ionization rises from a few percent just outside the zeroth fringe contour to values in the range 50 - 70% near the center of the arc.

c. Estimates of thermalization times for electron-atom and electron-ion collisions show that local thermal equilibrium should be well approximated everywhere except near the arc boundary P.

d. Assumption that the head shock is initiated by a one-dimensional adiabatic expansion of a hot cylindrical plasma formed by the peripheral arc, leads to an estimated mean temperature of the plasma

of about 25,000 ^{o}K (2.5 ev). Identification of the weak shock wave WS with a sound speed disturbance of the plasma yields almost the same mean temperature in the plasma.

e. Finally, consideration of conditions immediately behind the leading arc boundary P, indicates that thermal equilibrium between electrons and ions does not hold, that electron temperatures as high as 200 ev may occur, and that the arc boundary may reasonably be thought of as a shock wave of the electron driven type.

F. D. BENNETT

BIBLIOGRAPHY

1. Bennett, F. D. and Shear, D. D. "Shock Waves Exploding Wires at Low Ambient Densities". BRL Report No. 1152 (October 1961). See also Proceedings of the Conference on Exploding Wires; Boston, Massachusetts (November 1961) to be published.

2. Alpher, R. A. and White, D. R. Phys. Fluids 2, 162 (1959)

3. Lin, S. C. J. Appl. Phys. 25, 54 (1954)

4. Gerber, N. and Bartos, J. M. "Tables of Cylindrical Blast Functions for $\gamma = 5/3$ and $\gamma = 7/5$", BRL Memo Report No. 1376 (September 1961), Aberdeen Proving Ground, Maryland

5. Fowler, R. G., Paxton, G. W. and Hughes, H. G., Phys. Fluids, 4, 234 (1961); Fowler, R. G. and Fried, B. D., Phys. Fluids 4, 767 (1961).

6. Brown, S. C. Basic Data of Plasma Physics, (Technology Press of M.I.T. and John Wiley and Sons, Inc., New York, 1959) pp 1-7.

7. Bennett, F. D., Burden, H. S. and Shear, D. D. "Correlated Electrical and Optical Measurements of Exploding Wires". BRL Report No. 1133 (Aberdeen Proving Ground, Maryland, June 1961). Also Phys. Fluids 5, 102 (1962).

8. Spitzer, L., Jr. "Physics of Fully Ionized Gases", (Interscience Publishers, Inc., New York 1956) pp 78 - 80.

9. Resler, E. L., Lin, S. C. and Kantrowitz, A. R. J. Appl. Phys. 23, 1390 (1952).

10. Olsen, H. N., Phys. Fluids 2, 614 (1959).

11. Reference 8, p.61.

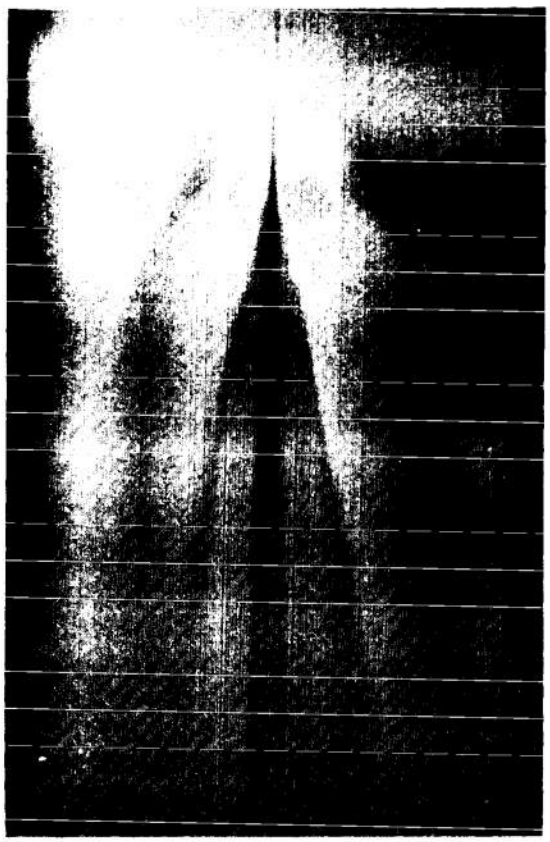

Fig. 1 Single Fringe Streak Interferogram.
4 mil Cu wire at 20 kv, 1/32-atm argon.

Fig. 2 Single Fringe Streak Interferogram.
4-mil Cu. Wire at 20 kv, 1/16-atm argon.

Fig. 3 Single Fringe Streak Interferogram.
4-mil Cu wire at 20 kv, 1/8-atm argon.

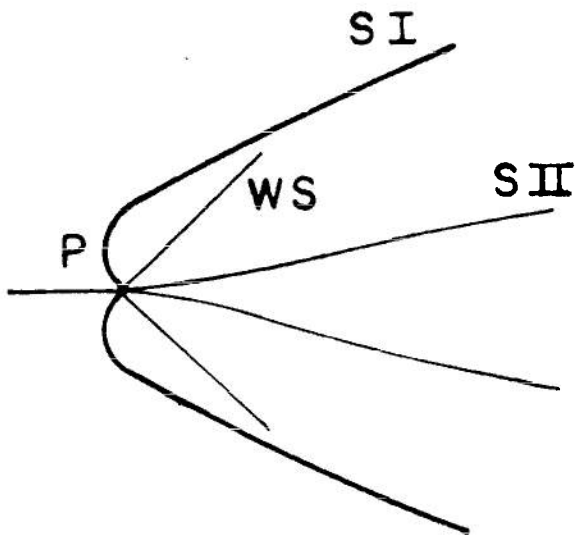

Fig. 4 Diagram of Shock Wave Locations.

DISTRIBUTION LIST

No. of Copies	Organization
10	Commander Armed Services Technical Information Agency ATTN: TIPCR Arlington Hall Station Arlington 12, Virginia
2	Chief of Ordnance ATTN: ORDTB - Bal Sec ORDTN Department of the Army Washington 25, D.C.
2	Commanding General Frankford Arsenal ATTN: Mr. Charles Lukens - Bldg. 150 Library Branch, 0270, Bldg. 40 Philadelphia 37, Pennsylvania
3	Commanding Officer Picatinny Arsenal ATTN: Feltman R&E Laboratories NASL Mr. S.S. Verner Dover, New Jersey
2	Commanding General U.S. Army Ordnance Missile Command ATTN: Deputy Commanding General for Ballistic Missiles - Dr. T.A. Barr Director, Research & Development Redstone Arsenal, Alabama
1	Commanding Officer Diamond Ordnance Fuze Laboratories ATTN: Technical Information Office - Branch 012 Washington 25, D.C.
1	Commanding Officer Army Research Office (Durham) Ordnance Liaison Group ATTN: Mr. J.R. Lane Box CM, Duke Station Durham, North Carolina
1	Army Research Office Arlington Hall Station Arlington, Virginia
3	Chief, Bureau of Naval Weapons ATTN: DIS-33 Department of the Navy Washington 25, D.C.
1	Commander Naval Ordnance Laboratory ATTN: Library White Oak, Silver Spring 19, Maryland
1	Commander U.S. Naval Ordnance Test Station ATTN: Technical Library China Lake, California
1	Superintendent U.S. Naval Postgraduate School Monterey, California
3	Director U.S. Naval Research Laboratory ATTN: Dr. E.A. McLean Dr. S.A. Ramsden Dr. A.C. Kolb Washington 25, D.C.
1	Commander U.S. Naval Weapons Laboratory Dahlgren, Virginia
1	Commander Air Proving Ground Center ATTN: PGAPI Eglin Air Force Base, Florida
	Of Interest to: PGEM

DISTRIBUTION LIST

No. of Copies	Organization
3	Commander Air Force Cambridge Research Laboratory ATTN: W.G. Chace - CRZN M.A. Levine M. O'Day L.G. Hanscom Field Bedford, Massachusetts
1	Commander Air Force Special Weapons Center ATTN: SWRP Kirtland Air Force Base, New Mexico
1	Director Air University Library ATTN: AUL (3T-AUL-60-118) Maxwell Air Force Base, Alabama
1	Commander Aeronautical Systems Division ATTN: WWAD Wright-Patterson Air Force Base, Ohio
1	Director National Aeronautics and Space Administration 1520 H Street, N.W. Washington 25, D.C.
2	Director National Aeronautics and Space Administration ATTN: Mr. V.J. Stevens Mr. Harvey Allen Ames Research Center Moffett Field, California
1	Director National Aeronautics and Space Administration Langley Research Center Langley Field, Virginia
1	Director National Aeronautics and Space Administration Lewis Research Center Cleveland Airport Cleveland, Ohio
3	Director National Bureau of Standards ATTN: D.H. Tsai J.H. Park Mr. Paul H. Krupenie 232 Dynamometer Building Washington 25, D.C.
1	U.S. Atomic Energy Commission ATTN: Technical Reports Library Mrs. J. O'Leary for Division of Military Applications Washington 25, D.C.
3	U.S. Atomic Energy Commission Los Alamos Scientific Laboratory ATTN: Dr. J.L. Tuck Dr. R.G. Schreffler Dr. R.E. Duff P.O. Box 1663 Los Alamos, New Mexico
1	Jet Propulsion Laboratory ATTN: Mr. Irl E. Newlan - Reports Group 4800 Oak Grove Drive Pasadena, California
1	Cornell Aeronautical Laboratory, Inc. ATTN: Mr. Joseph Desmond, Librarian 4455 Genessee Street Buffalo 5, New York

DISTRIBUTION LIST

No. of Copies	Organization
2	General Electric Research Laboratory ATTN: Dr. R.A. Alpher Dr. D.R. White P.O. Box 1088 Schenectady, New York
1	California Institute of Technology Aeronautics Department ATTN: Professor H.W. Liepmann 1201 East California Street Pasadena 4, California
1	California Institute of Technology Guggenheim Aeronautical Laboratory ATTN: Professor L. Lees Pasadena 4, California
1	Case Institute of Technology Department of Mechanical Engineering ATTN: Professor G. Kuerti University Circle Cleveland 6, Ohio
1	Cornell University Graduate School of Aeronautical Engineering ATTN: Professor E.L. Resler Ithaca, New York
1	Harvard Observatory Harvard University ATTN: Professor F.L. Whipple Cambridge 38, Massachusetts
1	Applied Physics Laboratory The Johns Hopkins University 8621 Georgia Avenue Silver Spring, Maryland
1	The Johns Hopkins University Department of Aeronautics ATTN: Professor L.S.G. Kovaszny Baltimore 18, Maryland
1	Lehigh University Department of Physics ATTN: Professor R.J. Emrich Bethlehem, Pennsylvania
1	Pennsylvania State University Physics Department ATTN: Professor R.G. Stoner State College, Pennsylvania
1	Princeton University Forrestal Research Center ATTN: Professor S. Bogdonoff Princeton, New Jersey
1	Princeton University ATTN: Professor Lyman Spitzer, Jr. Princeton, New Jersey
1	Stanford University Department of Mechanical Engineering ATTN: Professor D. Bershader Stanford, California
1	Syracuse University Department of Physics ATTN: Professor C.H. Bachman Syracuse 10, New York
1	University of California Low Pressures Research Project ATTN: Professor S.A. Schaaf Berkeley 4, California
2	University of California Department of Chemistry ATTN: Dr. C.P. Nash Dr. W.G. McMillan Los Angeles, California
1	University of Chicago The Enrico Fermi Institute of Nuclear Studies ATTN: Professor E.N. Parker Chicago 37, Illinois
1	University of Illinois Aeronautical Institute ATTN: Professor B.L. Hicks Urbana, Illinois

DISTRIBUTION LIST

No. of Copies	Organization
2	University of Maryland Institute for Fluid Dynamics And Applied Mathematics ATTN: Professor S.I. Pai Professor J.M. Burgers College Park, Maryland
1	University of Michigan Department of Physics ATTN: Professor Otto Laporte Ann Arbor, Michigan
1	University of Michigan Willow Run Laboratories P.O. Box 2008 Ann Arbor, Michigan
1	University of Oklahoma Department of Physics ATTN: Professor R.G. Fowler Norman, Oklahoma
1	University of Pennsylvania Moore School of Electrical Engineering ATTN: Professor S. Gorn Philadelphia, Pennsylvania
1	Dr. G.W. Anderson Sandia Corporation Sandia Base P.O. Box 5800 Albuquerque, New Mexico
1	Professor J.W. Beams University of Virginia Department of Physics McCormic Road Charlottesville, Virginia
1	Professor R.C. Binder University of Southern California Engineer Center University Park Los Angeles 7, California
1	Professor W. Bleakney Princeton University Palmer Physical Laboratory Princeton, New Jersey
1	Professor J. Lloyd Bohn Temple University Department of Physics Philadelphia, Pennsylvania
1	Professor R.G. Campbell Hartford Graduate Center R.P.I. East Windsor Hill, Connecticut
1	Mr. Paul R. Carson Research Assistant Brown University Engineering Division Providence, Rhode Island
1	Professor G.F. Carrier Harvard University Division of Engineering and Applied Physics Cambridge 38, Massachusetts
1	Professor R.H. Cole Brown University Department of Chemistry Providence, Rhode Island
1	Professor R.L. Chuan University of Southern California Engineering Center Los Angeles 7, California
1	Dr. Eugene C. Cnare Sandia Corporation Sandia Base P.O. Box 5800 Albuquerque, New Mexico

DISTRIBUTION LIST

No. of Copies	Organization
1	Mr. Robert Dennen Armour Research Foundation Illinois Institute of Technology Center Chicago 16, Illinois
1	Professor H.W. Emmons Harvard University Cambridge 38, Massachusetts
1	Dr. H.W. Hendel Radio Corporation of America Laboratories Princeton, New Jersey
1	Miss Margaret W. Imbrie E.I. DuPont de Nemours & Company Eastern Laboratory Library Drawer G Gibbstown, New Jersey
1	Dr. G. Sargent Janes AVCO Manufacturing Corporation Research & Advanced Development Div. 2385 Revere Beach Parkway Everett 49, Massachusetts
1	D.L. Jones National Bureau of Standards Boulder, Colorado
1	Professor G.B. Kistiakowsky Harvard University Department of Chemistry 12 Oxford Street Cambridge 38, Massachusetts
1	Professor L.B. Loeb University of California Department of Physics Berkeley, California
1	Dr. R.C. Maninger General Precision Laboratory, Inc. 63 Bedford Road Pleasantville, New York
1	Dr. Earle B. Mayfield U.S. Naval Ordnance Test Station Michelson Laboratory China Lake, California
1	Dr. Frank W. Neilson Sandia Corporation Sandia Base P.O. Box 5800 Albuquerque, New Mexico
1	Dr. A.E. Puckett Hughes Aircraft Company Culver City, California
1	Professor E.M. Pugh Carnegie Institute of Technology Department of Physics Pittsburgh 13, Pennsylvania
1	Dr. R.J. Reithel University of California Los Alamos Scientific Laboratory Los Alamos, New Mexico
1	Mr. Zoltan Rieder Yeshiva University Graduate School of Mathematical Sciences Amsterdam Avenue & 186th Street New York 33, New York
1	Dr. Carl A. Rouse University of California Lawrence Radiation Laboratory Theoretical Division P.O. Box 808 Livermore, California
1	Dr. G.T. Skinner Cornell Aeronautical Laboratory, Inc. 4455 Genessee Street Buffalo 5, New York
1	Mr. W.L. Staff Lockheed Aircraft Corporation Missiles & Space Division Palo Alto, California

DISTRIBUTION LIST

No. of Copies	Organization
1	Dr. Alvin Tollestrup California Institute of Technology Pasadena 4, California
1	Dr. T.J. Tucker Sandia Corporation Sandia Base P.O. Box 5800 Albuquerque, New Mexico
1	I.M. Vitkovitsky U.S. Naval Research Laboratory Washington 25, D.C.
1	Mr. E.E. Walbrecht Picatinny Arsenal Explosive Research Section Dover, New Jersey
1	Dr. Francis H. Webb California Institute of Technology Pasadena 4, California
1	Dr. L. Zernow Aerojet-General Corporation 6352 North Irwindale Road Azusa, California
4	Defence Research Member Canadian Joint Staff 2450 Massachusetts Avenue, N.W. Washington 8, D.C.
11	The Scientific Information Officer Defence Research Staff British Embassy 3100 Massachusetts Avenue, N.W. Washington 8, D.C 1 copy for retransmittal to: Dr. A. Watson Research Department Arc Physics Section Associated Electrical Industries, Ltd. Trafford Park Manchester 17, England

AD ______ Accession No. ______ UNCLASSIFIED

Ballistic Research Laboratories, APG
SHOCK PRODUCING MECHANISMS FOR EXPLODING WIRES
F. D. Bennett

Exploding wires
Shock waves

BRL Report No. 1161 February 1962

DA Proj No. 503-03-001, OMSC No. 5010.11.814
UNCLASSIFIED Report

Single fringe interferograms are presented of 4-mil Cu wires exploded at 20 kv into argon at ambient pressures of 1/8, 1/16 and 1/32 atm. Features discernible include a compressive head shock wave, arc plasma, a weak plasma wave and the expanding metal wire. On the basis of certain plausible assumptions it is seen that the arc plasma has a temperature of about 2.5 ev; but its leading edge, a region not in thermal equilibrium, has electron temperatures $\sim 10^2$ ev and is the boundary of an electron driven shock wave.

AD ______ Accession No. ______ UNCLASSIFIED

Ballistic Research Laboratories, APG
SHOCK PRODUCING MECHANISMS FOR EXPLODING WIRES
F. D. Bennett

Exploding wires
Shock waves

BRL Report No. 1161 February 1962

DA Proj No. 503-03-001, OMSC No. 5010.11.814
UNCLASSIFIED Report

Single fringe interferograms are presented of 4-mil Cu wires exploded at 20 kv into argon at ambient pressures of 1/8, 1/16 and 1/32 atm. Features discernible include a compressive head shock wave, arc plasma, a weak plasma wave and the expanding metal wire. On the basis of certain plausible assumptions it is seen that the arc plasma has a temperature of about 2.5 ev; but its leading edge, a region not in thermal equilibrium, has electron temperatures $\sim 10^2$ ev and is the boundary of an electron driven shock wave.

AD ______ Accession No. ______ UNCLASSIFIED

Ballistic Research Laboratories, APG
SHOCK PRODUCING MECHANISMS FOR EXPLODING WIRES
F. D. Bennett

Exploding wires
Shock waves

BRL Report No. 1161 February 1962

DA Proj No. 503-03-001, OMSC No. 5010.11.814
UNCLASSIFIED Report

Single fringe interferograms are presented of 4-mil Cu wires exploded at 20 kv into argon at ambient pressures of 1/8, 1/16 and 1/32 atm. Features discernible include a compressive head shock wave, arc plasma, a weak plasma wave and the expanding metal wire. On the basis of certain plausible assumptions it is seen that the arc plasma has a temperature of about 2.5 ev; but its leading edge, a region not in thermal equilibrium, has electron temperatures $\sim 10^2$ ev and is the boundary of an electron driven shock wave.

AD ______ Accession No. ______ UNCLASSIFIED

Ballistic Research Laboratories, APG
SHOCK PRODUCING MECHANISMS FOR EXPLODING WIRES
F. D. Bennett

Exploding wires
Shock waves

BRL Report No. 1161 February 1962

DA Proj No. 503-03-001, OMSC No. 5010.11.814
UNCLASSIFIED Report

Single fringe interferograms are presented of 4-mil Cu wires exploded at 20 kv into argon at ambient pressures of 1/8, 1/16 and 1/32 atm. Features discernible include a compressive head shock wave, arc plasma, a weak plasma wave and the expanding metal wire. On the basis of certain plausible assumptions it is seen that the arc plasma has a temperature of about 2.5 ev; but its leading edge, a region not in thermal equilibrium, has electron temperatures $\sim 10^2$ ev and is the boundary of an electron driven shock wave.